

---

## **Simultaneous Transport of Water and Organic Molecules through Polyelectrolyte Membranes**

---

**D. Rivin, G. Meermeier, N. S. Schneider, A. Vishnyakov, and A. V. Neimark**

USA RDECOM (Natick Soldier Center), Natick, Massachusetts, and Center for Modeling and Characterization of Nanoporous Materials, TRI/Princeton, 601 Prospect Avenue, Princeton, New Jersey 08542

The Journal of  
**Physical Chemistry B<sup>®</sup>**

Reprinted from  
Volume 108, Number 26, Pages 8900–8909

# Simultaneous Transport of Water and Organic Molecules through Polyelectrolyte Membranes

D. Rivin,<sup>\*,†</sup> G. Meermeier,<sup>†</sup> N. S. Schneider,<sup>†</sup> A. Vishnyakov,<sup>‡</sup> and A. V. Neimark<sup>\*,‡</sup>

USA RDECOM (Natick Soldier Center), Natick, Massachusetts, and Center for Modeling and Characterization of Nanoporous Materials, TRI/Princeton, 601 Prospect Avenue, Princeton, New Jersey 08542

Received: November 12, 2003; In Final Form: April 14, 2004

Polyelectrolyte membranes (PEM) such as Nafion (Du Pont) used as compartment separators in fuel cells and other electro-chemical applications are also of interest as permselective diffusion barriers in protective fabrics. By means of sorption and permeation experiments in conjunction with molecular dynamics simulations, we explore the permeability of Nafion membrane to water and hydrophilic solvents such as 1-propanol and dimethyl methylphosphonate, focusing on the relationship between polymer structure, solvation, and solvent diffusion. It is shown that the composition of the solvent strongly affects the membrane permeability, which cannot be predicted purely from permeability measurements with pure components. This effect is related to a complex microphase segregation in the membranes swollen in aqueous solutions of polar solvents. The results obtained demonstrate possible mechanisms of the diffusion of alcohols and alkyl-phosphonates in hydrated ionomer membranes and reveal properties controlling the utilization of PEM for protective fabrics.

## I. Introduction

Due to high water vapor permeability, chemical and thermal stability, mechanical strength, and blocking action with respect to organic vapors and colloids, polyelectrolyte membranes (PEM) open up new prospects for producing novel protective clothing materials with superior protection and comfort properties to replace currently available commercial materials such as air-permeable fabrics containing activated carbon. A perfluoro-ionomer, Nafion, is of particular interest because of its exceptionally high water vapor transport, promoted by sulfonic acid terminated perfluoroether side chains. The physical properties of Nafion are largely determined by the microphase segregation into a hydrophilic subphase formed by the side chains, water (and/or other hydrophilic components) and counterions, and a hydrophobic phase formed by the perfluorocarbon backbone that contains a small amount of crystallinity.<sup>1,2</sup> Details of the structure and transport mechanism for water and organic species continue to be a subject of controversy.<sup>3,4</sup>

It was expected that the presence of ionic regions that promote transport of water in a fully fluorinated composition might lead to favorable permselective barrier properties for various classes of organic molecules, including chemical warfare agents. Nafion in its commercial acid form exhibits preferential permeation of water compared to the nerve agent simulant, dimethylmethylphosphonate (DMMP). Substitution with cations enhances the permselectivity of Nafion significantly. In fact, separately determined permeation rates of water vapor and DMMP vapor in Nafion modified with multivalent cations indicate a remarkable improvement in barrier performance with only a modest reduction in water vapor permeability. At the same time, separately determined permeabilities are not a sufficient test of permselective performance, since barrier properties may be

influenced by interactions between water and the organic permeant and changes in phase morphology induced by either component. So far, the effect of sorbate–sorbate interactions on transport behavior of dual penetrants has received little attention, mostly dealing with vapor concentration of one of the penetrant liquids.<sup>5–7</sup>

We present the results of sorption and permeation experiments on binary mixtures of water with DMMP (aprotic hydrophilic solvent, a nerve agent simulant), and water with 1-propanol (hydrogen bonding protic solvent) of different compositions in Nafion acid membranes and those substituted with multivalent counterions. To explain the experimental results and understand the underlying mechanisms of DMMP diffusion in Nafion, we perform molecular dynamics (MD) simulations of individual Nafion side chains and thin films in water, DMMP, and water–DMMP mixtures.

## II. Experimental Section

**II.1. Materials.** Nafion films of equivalent weight 1100, in thicknesses of 178  $\mu\text{m}$  (Nafion 117) and 51  $\mu\text{m}$  (Nafion 112), were obtained from CG Processing, Inc. All films were pretreated with aqua regia at 60 °C and then washed with deionized water to remove impurities and ensure complete conversion to the acid. Calcium ion substitution of Nafion 112 was carried out by immersion in 0.35 molar  $\text{Ca}(\text{NO}_3)_2$  for 68 h at room temperature followed by washing three times in deionized water and drying at 110 °C. Ferric ion substitution was carried out by immersion in 0.9 M  $\text{FeCl}_3$  at room temperature, followed by a similar work up. The acid form is designated as NafionH, and the salts are designated as NafionCa and NafionFe. Dimethyl methylphosphonate (97%) and 1-propanol (99.5%) were obtained from Sigma-Aldrich and dried over molecular sieve 4a before use. Quantitative proton replacement was obtained for both substituted membranes as determined by prompt gamma neutron activation analysis.<sup>8</sup> From the cation/sulfur ratios of  $0.50 \pm 0.003$  for divalent calcium and  $0.37 \pm$

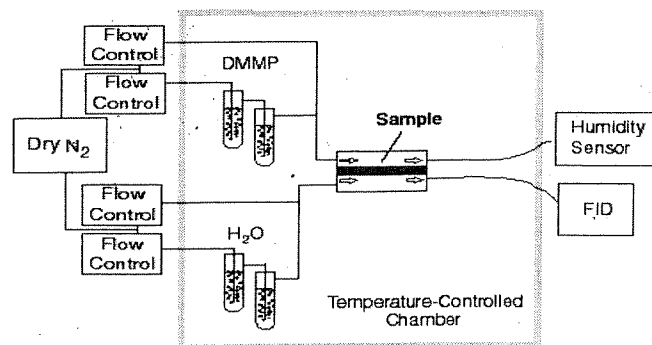


Figure 1. Apparatus for permeation measurements.

0.004 for trivalent iron, it appears that both ions provide the stoichiometric number of ionic cross-links between sulfonate groups.

**II.2. Sorption and Permeation Measurements.** Immersion sorption concentrations were determined gravimetrically on blot dried samples. Measurements were repeated until a steady-state concentration had been achieved. Vapor sorption was conducted with films placed in a tube and exposed to a stream of mixed vapor. Total sorption of aqueous DMMP was determined by weight loss of water over molecular sieves, followed by extraction of DMMP with water, drying at 105 °C, and then reweighing. Water and propanol concentrations were determined by thermal desorption followed by GC analysis. The volume fraction of sorbate is calculated from weight percent uptake using a Nafion density of 1.95 g/cm<sup>3</sup> and densities of 1.15 and 0.804 g/cm<sup>3</sup> for DMMP and propanol, respectively.

Permeation measurements were conducted at atmospheric pressure over a range of selected vapor activities ( $P/P_0$ ), generated by mixing saturated vapor from a bubbler with a dry nitrogen diluent stream, in ratios set with electronic mass flow controllers. In countercurrent flow, water vapor and organic vapor feed streams entered on opposite sides of the membrane (Figure 1), whereas a single mixed feed stream was used in co-current flow. The permeation cell exposes a rectangular sample area, 1.91 cm × 3.18 cm, with the membrane forming a pressure seal between the two halves of the cell. Flow rates for challenge and sweep were 60 cm<sup>3</sup>/min. Bubblers and permeation cell were housed in a constant temperature cabinet maintained at 30 ± 0.1 °C. The permeation flux is reported in kg/day m<sup>2</sup> for water and g/day m<sup>2</sup> for DMMP or propanol.

### III. Sorption and Permeation of DMMP and Water

**III.1. Sorption.** The dry NafionH membrane sorbs 133 wt % of pure DMMP (volume fraction  $V_D = 0.71$ ), that is much higher than the maximum sorption of water (22 wt %,  $V_{H_2O} = 0.32$ ) or propanol (59 wt %,  $V_{PrOH} = 0.61$ ). This difference in solubility arises from solvent interactions with different regions of the polymer. In earlier simulation studies<sup>9</sup> of the solvation of Nafion side chains in water and methanol, it was observed that, in addition to intense interactions with the  $-SO_3^-$  groups via hydrogen bonds, the alcohol (in contrast to water) also interacts with the hydrophobic backbone via van der Waals forces. NMR studies with ethanol<sup>10</sup> also confirmed swelling and increased mobility of presumably amorphous fluorocarbon regions due to solvation by ethanol (and by analogy, propanol). However, DMMP was found to concentrate selectively around the fluoroether side chains<sup>11</sup> without solvating the fluorocarbon region.

Results of the immersion sorption of binary mixtures of DMMP and water by NafionH are shown in Figure 2a. Total

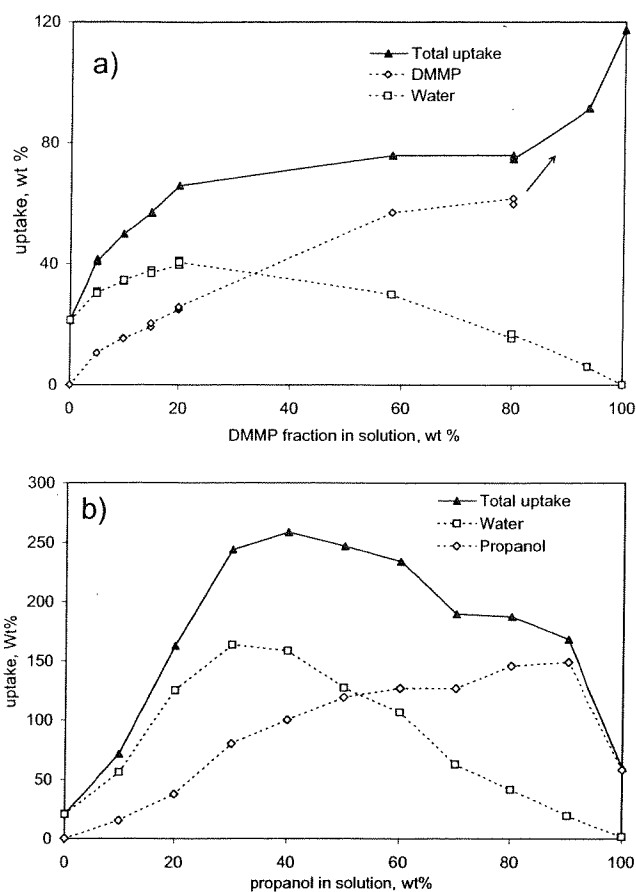
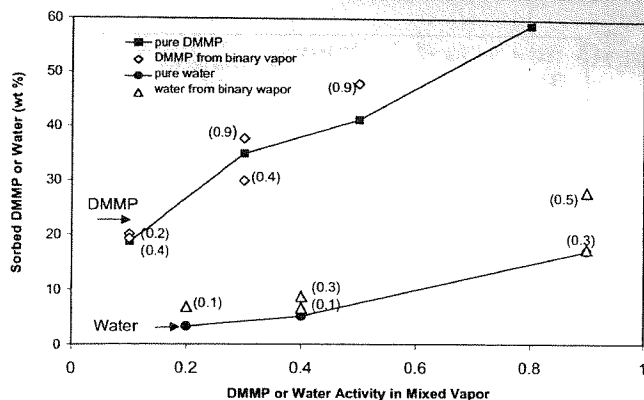


Figure 2. Sorption isotherms of water and hydrophilic organic solvents DMMP (a) and propanol (b) in NafionH from aqueous solution of the organic solvents at 298 K.

uptake increases almost linearly with DMMP solution weight fraction,  $W_D < 0.2$ , but changes very little at  $0.2 > W_D < 0.8$ . However, as  $W_D$  approaches 1, the total sorption increases rapidly to the saturation concentration of 133 wt % in the film. Initial water uptake increases rapidly, exhibits a broad maximum with a water concentration of 40% (twice the saturation concentration for pure water), and exceeds the saturation concentration to  $W_D = 0.7$ . The molar ratio of water to DMMP,  $R_{WD}$ , is smaller in the sorbed composition than in the mixed liquid up to the maximum, where the values are  $R_{WD} = 11$  and 28 for uptake and immersion liquid, but approach the liquid  $R_{WD}$  at higher solution concentrations. At the same time, DMMP sorption increases monotonically, with a nearly constant slope up to  $W_D \approx 0.6$ , is almost constant at  $0.6 < W_D < 0.8$ , and then increases rapidly to saturation in pure DMMP. At  $0.2 < W_D < 0.8$ , the increase of DMMP sorption offsets the decrease in water sorption; thus, the total sorption is constant.

To understand better the mechanisms of sorption from the binary mixture, we explored the influence of water activity on sorption of DMMP. Sorption data from the mixed vapor at 0.1–0.5 activity of DMMP and 0.2–0.9 activity of water are compared to values from equilibrium sorption isotherms for the pure vapors in Table 1 and Figure 3. Water sorption from the mixed vapor is moderately higher than isotherm values for pure water at all concentrations of DMMP and the increase is somewhat greater at high DMMP activity. The presence of water has little effect on DMMP sorption except for a small increase at high water activity. Values of  $R_{WD}$  are much higher in the mixed vapor than in the sorbed composition, similar to the trend with the liquid mixture at low DMMP concentrations. In general, interaction effects do not alter solubility significantly for either



**Figure 3.** Sorption of DMMP and water from one- and two-component vapors in NafionH at 298 K. The numbers in brackets shows the activity ( $P/P_0$ ) of the second component.

**TABLE 1: Sorbed Composition from DMMP/Water Mixed Vapor**

	Vapor Mixture				
DMMP activity	0.1	0.1	0.3	0.3	0.5
water activity	0.2	0.4	0.4	0.9	0.9
molar ratio	56.2	112.3	37.4	84.2	50.5
	Uptake Predicted from Initial Isotherms				
DMMP wt %	18.7	18.7	34.9	34.9	41.2
water wt %	3.2	5.0	5.0	16.7	16.7
	Uptake Actual				
DMMP, wt %	20.1	19.3	29.9	37.7	47.9
water, wt %	6.8	6.6	8.7	17.4	28
molar ratio	2.3	2.4	2	3.2	4

DMMP or water for sorption from mixed vapor at sorbed concentrations, which are well below the maximum capacity attained upon liquid immersion.

**III.2. Permeability.** Apparent values of water flux in the Nafion117H membrane increase from 0.80 to 5.16 kg/m<sup>2</sup> day over the activity range 0.2–0.9. However, correction for the boundary layer resistance is necessary to accurately determine the effect of changing conditions on membrane permeability.<sup>12</sup> As a result of the low resistance of NafionH to water, the boundary layer resistance causes a large decrease in net flux. The change is greatest at the highest activity since membrane resistance decreases with increasing water activity. Boundary corrected fluxes for water, in Table 2 and Figure 4a, increase rapidly with activity from 1.25 kg/m<sup>2</sup> day at activity 0.2 to 16.5 kg/m<sup>2</sup> day at activity 0.9. Introduction of DMMP vapor causes a 3.5-fold reduction in water flux for all values of water activity (0.2–0.9). The effect is essentially independent of DMMP activity over the measured range, 0.1–0.5, and independent of the relative direction of permeation. The large reduction in water flux caused by DMMP, observed even at low DMMP activities, was not expected as water sorption increases in the presence of DMMP. At the same time, Figure 5a shows that water vapor has little effect on the flux of DMMP in countercurrent permeation, but in co-current flow, the DMMP flux strongly increases with water activity and is relatively independent of DMMP activity.

Ca<sup>2+</sup> and Fe<sup>3+</sup> modifications of Nafion have been shown to be excellent barriers to DMMP in sorption and permeation measurements carried out in the absence of water.<sup>13</sup> Permeation results with NafionCa and NafionFe are compared to those for NafionH in Table 3. Whereas 178 μm (Nafion 117) films were used in all but one of the measurements with NafionH, 51 μm (Nafion 112) films of the exchanged membranes were required in order to obtain a sufficient flux of DMMP for accurate

**TABLE 2: Flux for DMMP–Water and Propanol–Water Mixtures**

flow direction	organic component activity, $P/P_0$	water activity, $P/P_0$	water flux, $J_{H_2O}$ , kg/m <sup>2</sup> day	organic component flux, $J_{DMMP/PrOH}$ , g/m <sup>2</sup> day
	Organic Component: DMMP			
	0	0.2	1.25	
	0	0.3	2.00	
	0	0.5	6.33	
	0	0.8	14.07	
	0	0.9	16.49	
	0.1	0		187
	0.3	0		335
	0.5	0		689
co-current	0.1	0.2	0.46	648
co-current	0.1	0.4	0.92	1742
co-current	0.3	0.3	0.82	970
co-current	0.3	0.4	1.18	1670
counter	0.1	0.4	0.79	599
counter	0.1	0.9	4.11	280
counter	0.3	0.3	0.73	493
counter	0.3	0.4	1.06	488
counter	0.3	0.5	1.49	449
counter	0.3	0.9	4.78	415
counter	0.5	0.4	1.06	749
counter	0.5	0.8	4.52	627
counter	0.5	0.9	5.10	524
	Organic Component: 1-propanol			
	0.3	0		791
	0.5	0		1737
	0.9	0		5387
co-current	0.5	0.3	0.47	2975
co-current	0.3	0.5	1.51	n.d
counter	0.3	0.5	1.36	1413
counter	0.9	0.5	1.05	7187
counter	0.5	0.3	0.43	2092
counter	0.5	0.5	1.15	2566
counter	0.5	0.9	3.62	4283

measurement. In the absence of water, the flux of DMMP at activity 0.5 is reduced from 689 g/m<sup>2</sup> day in Nafion117H to 3 g/m<sup>2</sup> day in Nafion112Ca and is not detectable in Nafion112Fe. This improvement in barrier performance is maintained up to water activities of 0.5 in NafionCa and to 0.7 in NafionFe. However, at water activity 0.9, DMMP flux in both cation-modified membranes is in the same range as that of Nafion117H. Substitution with multivalent cations also reduces water permeability, as illustrated by the reduction shown for NafionCa from 16.5 to 3.80 kg/m<sup>2</sup> day at water activity 0.9. There is an additional decrease in water flux for both modified membranes in the presence of DMMP as observed with NafionH. In the next section, we examine the effect on transport behavior of the competition between water and a protic solvent, propanol, expected to interact with both polar and nonpolar portions of the polymer.

#### IV. Sorption and Permeation of Propanol and Water

**IV.1. Sorption.** Weight uptake in NafionH, determined by immersion sorption in mixed propanol water solutions, increases rapidly with propanol concentration reaching a broad maximum of 250 wt % at a propanol weight fraction,  $W_p$ , of 0.4 in the mixed liquid (Figure 2b). Initial swelling is dominated by the preferential uptake of water, which reaches a maximum greater than 160 wt % at  $W_p = 0.3$ , well above the solubility of 22 wt % for pure water, with a molar ratio of water to propanol of  $R_{WP} = 7$ . Strong interaction between the two liquids also promotes propanol solubility. At  $W_p = 0.9$ , propanol attains a

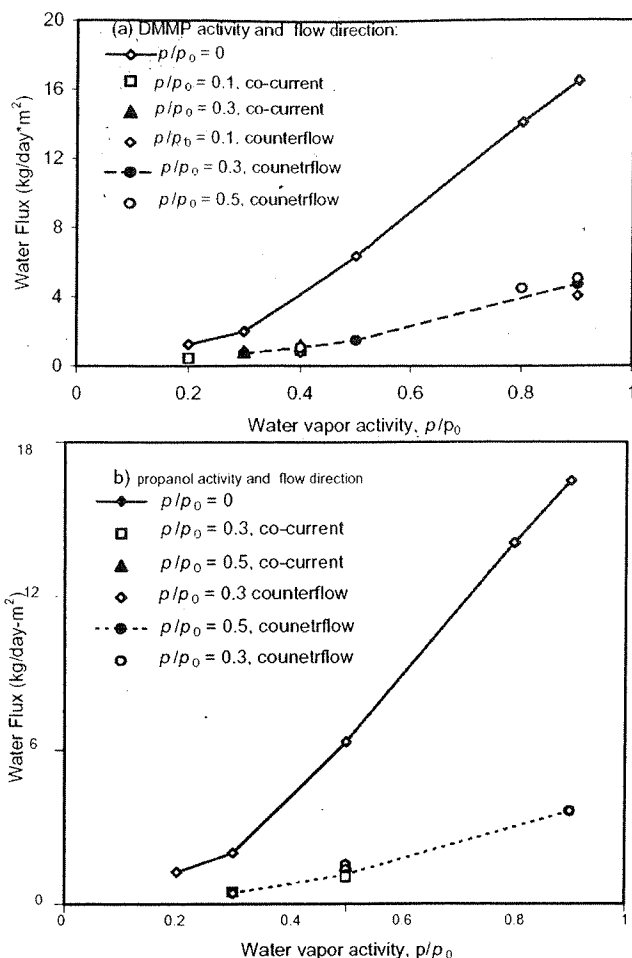


**Figure 4.** Influence of DMMP (a) and propanol (b) activities on the permeation of water through Nafion 117 membranes at 298 K.

maximum sorption of 150 wt %, exceeding the solubility of 59 wt % for dry propanol in NafionH. At maximum total uptake,  $R_{WP} = 5$ . It is notable that  $R_{WP}$  values in the mixed liquid and in the sorbed composition are essentially equal over nearly the entire range of solution concentrations. In contrast to the behavior in immersion, sorbed water concentrations from the mixed vapor, recorded in Table 4, are close to isotherm values and do not increase with propanol activity in the mixed vapor. Also, the sorption of propanol is about twenty five percent lower than determined with pure propanol vapor and insensitive to water activity. Values of  $R_{WP}$  in the mixed vapor and uptake are nearly equal but limited to values less than two, indicating that sorbed compositions are enriched in propanol as compared to sorption from the mixed liquid.

**IV.2. Permeability.** As shown in Figure 4b the presence of propanol in the vapor stream causes a moderately larger reduction (almost 5-fold) in the flux of water than does DMMP. The proportional decrease in water flux is independent of the activity for either vapor (0.3–0.9) and slightly greater for co-current flow. The effect of water on the flux of propanol is equally dramatic as shown in Figure 5b. For countercurrent flow, the flux of propanol at 0.5 water activity is nearly doubled at the lowest propanol concentration and increased by one-third at the highest propanol concentration. The set of points at 0.5 propanol activity provide a comparison of the effect of water activity and permeation mode. In co-current flow, propanol flux increases by almost a factor of 2 at 0.3 activity water. In countercurrent flow, propanol flux increases progressively when

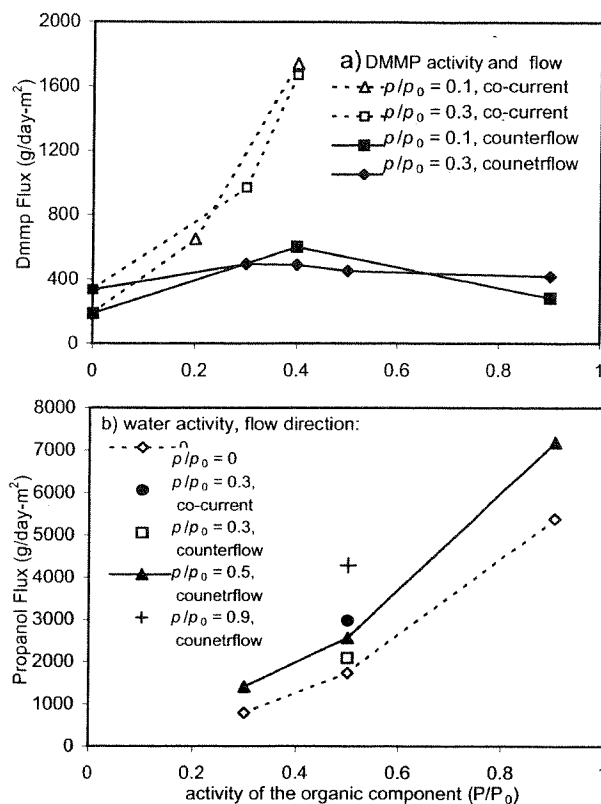


**Figure 5.** Influence of water on the permeation of DMMP (a) and propanol (b) through Nafion 117 membranes.

**TABLE 3: Effect of Cation Modification on Flux in Opposed Flow in Nafion 112 with Different Counterions**

counterion	DMMP activity, $P/P_0$	water activity, $P/P_0$	water flux, $J_{H_2O}$ , kg/m <sup>2</sup> day	DMMP flux, $J_{DMMP}$ , g/m <sup>2</sup> day
H <sup>+</sup>	0.3	0.5	3.65	1943
Ca <sup>2+</sup>	0.5	0.9	5.10	524
Ca <sup>2+</sup>	0.5	0		3
Ca <sup>2+</sup>	0	0.4	0.47	
Ca <sup>2+</sup>	0	0.9	3.78	
Ca <sup>2+</sup>	0.3	0.5	0.36	8
Ca <sup>2+</sup>	0.5	0.4	0.47	16
Fe <sup>3+</sup>	0.5	0.9	2.85	447
Fe <sup>3+</sup>	0.3	0.5	<0.30	
Fe <sup>3+</sup>	0.3	0.7	0.52	6
Fe <sup>3+</sup>	0.3	0.9	1.75	103
Fe <sup>3+</sup>	0.5	0.9	3.92	709

**TABLE 4: Sorbed Composition from Propanol/Water Mixed Vapor**

	Vapor Mixture				
	0.3	0.5	0.9	0.5	0.5
propanol activity	0.3	0.5	0.9	0.5	0.5
water activity	0.5	0.5	0.5	0.3	0.8
molar ratio	1.86	1.11	0.62	0.67	2.00
	Uptake Predicted				
propanol wt %	15.7	18.5	35.8	18.5	18.5
water wt %	6.1	6.1	6.1	4.1	16.7
	Uptake Actual				
propanol, wt %	9.7	13.5	22.5	13.5	14.1
water, wt %	6.6	5.7	5.0	6.7	7.1
molar ratio	2.3	1.4	0.7	1.1	1.7

water activity increases from 0.3 to 0.9, but 0.9 water activity produces a dramatic increase in propanol flux, nearly a factor of 2.5.

The effect of water–propanol interactions are qualitatively similar to those observed with water–DMMP in the marked reduction in water flux with propanol, both in co- and coun-

tercurrent flow and a substantial increase in propanol flux in co-current flow but differ in the marked increase in propanol flux that also occurs in countercurrent flow. The results of the sorption and permeation measurements demonstrate that the interactions between water and the two organic liquids have strong effects that could not be predicted from measurements with individual components. In particular, the high permeability of the Nafion membrane to DMMP in the presence of water at high activity, even with multivalent cation modification, is clearly not due to an increase in DMMP solubility but arises either from a change in the mechanism of DMMP transport and/or Nafion morphology. Molecular simulations provide insight into the effect of water–DMMP interactions on the transport mechanism in Nafion as described in section V.

## V. Molecular Dynamics Simulations

**V.1. Simulation Setup.** To explore the interactions of Nafion and DMMP and the DMMP/water mixture, we performed a series of molecular dynamics simulations of individual Nafion side chains and Nafion films immersed in water and DMMP. For computational convenience, simulations utilize the  $K^+$  sulfonate rather than the  $Ca^{2+}$  or  $Fe^{3+}$  salts described in section III; however, our immersion studies show that solubility and transport properties of potassium salts of Nafion are qualitatively similar to those of the corresponding polyvalent cation salts. In simulations with individual side chains, four model side chains were put in a large solvent bath at  $T = 303$  K and  $P = 1$  atm. The solvent consisted of 256 DMMP molecules in simulation with pure DMMP and 900 water molecules in the simulation with pure water. For the simulation with the Nafion film, the mixed solvent consisted of 60 DMMP molecules + 460 water molecules. This is equivalent to a dissolved solvent uptake of 20 wt % DMMP and 22 wt % water. A second film simulation with more dilute DMMP was carried out using 42 DMMP molecules (14 wt %) and 664 water molecules (32 wt %). Simulations were performed in NPT ensemble at  $T = 303$  K and  $P = 1$  atm for 1 ns, and the statistics were collected over the last 600 ps. Other simulation details were identical to those of ref 9.

In simulations of thin Nafion films, the film was formed by six, four-unit Nafion oligomers similar to those considered in refs 9 and 14. Initially, the film was constructed in a  $34 \text{ \AA} \times 34 \text{ \AA} \times 25 \text{ \AA}$  cubic periodic box ( $\rho = 2.0 \text{ g/cm}^3$ , roughly the density of dry Nafion<sup>15</sup>) using Cerius2 amorphous builder<sup>16</sup> and equilibrated via a static energy optimization and an MD simulation in NVT ensemble at 298 K for 200 ps. The solvent bath was also obtained by preliminary 100 ps MD simulation of 180 DMMP molecules and four  $K^+$  counterions in a box that had a shape of a straight parallelepiped with  $34 \text{ \AA} \times 34 \text{ \AA}$  cross-section at  $\rho = 1.15 \text{ g/cm}^3$ , the density of liquid DMMP at 298K and 1 atm. Then Nafion and solvent were brought into contact. Thus, in the initial configuration, the  $SO_3^-$  groups and counterions were more or less randomly distributed in the film and solvent, respectively. The equilibration time was 800ps and then the statistics were collected over another 800ps.

**V.2. Molecular Models.** Water was represented by a rigid three-center SPC/E model,<sup>17</sup> that reproduces quite accurately the density, heat of evaporation, and diffusion in pure water at ambient temperatures. A 7-center united-atom potential model for DMMP was reported in our previous publication.<sup>18</sup> This model correctly reproduces conformations of DMMP molecules and physical properties of pure liquid DMMP and provides a qualitatively consistent and reasonable picture of the molecular structure of DMMP-water mixtures.

**TABLE 5: Torsion Parameters for the Sidechain<sup>a</sup>**

dihedral	$V_1$ , kJ/mol	$V_2$ , kJ/mol	$V_3$ , kJ/mol	$V_4$ , kJ/mol
OCC	0	0	5.777	0
SCCO	25.21	5.155	11.96	0
CCOC	4.92	-16.26	11.96	0
CCCO	-17.84	6.36	28.08	0
OCCO	-17.82	5.76	26.62	0
CCCC <sup>20</sup>	23.75	3.97	-5.82	-8.87

$$^a \Psi_{\text{TORS}}(\theta) = \frac{1}{2}V_1(1 + \cos \theta) + \frac{1}{2}V_2(1 - \cos 2\theta) + \frac{1}{2}V_3(1 + \cos 3\theta) + \frac{1}{2}V_4(1 - \cos 4\theta).$$

Nafion was presented by the united-atom model.<sup>19</sup> LJ parameters were fitted to represent the physical properties of simpler substances that contain the same fragments as Nafion. However, the potentials for dihedral angles and partial charges were changed slightly. The dihedral angles were described using the same functions as in ref:<sup>20</sup>  $\Psi_{\text{TORS}}(\theta) = \frac{1}{2}V_1(1 + \cos \theta) + \frac{1}{2}V_2(1 - \cos 2\theta) + \frac{1}{2}V_3(1 + \cos 3\theta) + \frac{1}{2}V_4(1 - \cos 4\theta)$ . The coefficients (see Table 5) were fitted to give the same potential functions as the united-atom force field.<sup>19</sup> Individual Nafion side chains were represented by the model molecules  $(CF_3)_2CFOCF_2CF(CF_3)OCF_2CF_2SO_3^-$ . The partial atomic charges, shown under the elements, are taken as described previously.<sup>19,21</sup> The hydrophobic end of this model side chain consists of the CF group, which belongs to the skeleton of the Nafion polymer and also the two  $CF_3$  groups in place of the  $CF_2$  groups of the skeleton neighboring the side chain. The partial charges used in the simulations of model side chains were also used in the simulations of Nafion films. The other fluorocarbon groups of the skeleton were assigned zero partial charges.

The optimized geometry of the Nafion side chain practically coincides with that obtained using the all-atom force field<sup>9</sup> and similar to that obtained in ab initio optimization but shows a trans S– $CF_2$ – $CF_2$ –O dihedral angle instead of a gauche angle as previously reported.<sup>4</sup> In all simulations, the counterion was potassium  $K^+$  modeled as a charged LJ sphere.<sup>22</sup>

**V.3. Molecular Dynamics Simulations: Individual Side Chains in DMMP and Binary Solution.** Since the side chains were not connected to a skeleton as in refs 9 and 14, they showed a substantially better flexibility than in our earlier simulations of Nafion oligomers in water, methanol, and water–methanol mixture.<sup>9,14</sup> The most flexible was the O–CF– $CF_2$ –O dihedral angle; five conformation transitions were observed over the 600 ps simulation course around these bonds. The other torsion angles were quite stiff.

It should be noted that DMMP turned out to be a poor solvent for  $K^+$  ion, which caused association of all four  $-SO_3^-K^+$  groups, although initially the counterions were randomly distributed in the solvent. The state of the  $-SO_3^-K^+$  groups was traced using OS–K radial distribution functions shown for some of the systems in Figure 6. In the associated state, the “head”  $-SO_3^-K^+$  group is a strong dipole that forms a distinct first solvation shell of DMMP molecules that are turned toward the potassium atoms with their OP groups. The associated state of  $-SO_3^-K^+$  groups enhances the attractive interactions between the side chain and the solvent. Should the salt be dissociated (as was observed in the simulation with pure water), the “head” groups would be solvophobic due to a strong repulsion between the negatively charged oxygen atoms and a weak van der Waals interaction of the  $O_S$  oxygens with the methyl groups of DMMP. The van der Waals contribution dominates the interactions between the solvent and the hydrophobic “tail”, causing DMMP molecules to turn with the methyl groups toward the side chain.

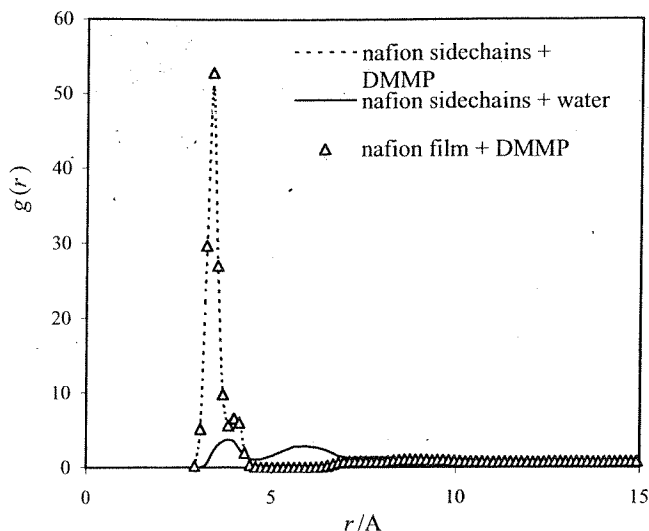


**Figure 6.**  $O_S$ -K radial distribution functions for model side chains in DMMP and thin Nafion film in pure DMMP, water, and DMMP-water mixture.

In the simulation with the mixed solvent, the contrast between the hydrophilic "head" and the hydrophobic "tail" caused a prominent segregation in the solvent into a hydrophilic subphase that consists of water and counterions and a hydrophobic subphase formed by DMMP (Figure 7). The hydrophilic "heads" are submerged in the hydrophilic subphase, whereas the "tails" of the side chains are submerged in the hydrophobic subphase. Thus, the model side chains serve as surfactant. All  $-SO_3^- K^+$  groups are dissociated, since the  $O_S$ -K RDF resembles closely that in pure water. Naturally, the counterions are located in the aqueous subphase as S-K RDF is practically the same as in water and drastically differs from that in DMMP.

Since DMMP and water are miscible, the scale of the segregation is limited, as in any surfactant solution. The system considered in our simulations is too small to estimate the segregation scale, and this problem is beyond the scope of this work. However, the simulation performed demonstrates that in PEM swollen in a mixed solvent the segregation may be more complex than in hydrated PEM. Certainly, the specific segregation in the mixture affects the mobilities of water and DMMP.

**V.4. Molecular Dynamics Simulations: Thin Nafion Films in Water and DMMP.** After the 1.6 ns simulations, the Nafion-DMMP system still had lamella morphology with a thin film of polymer surrounded by DMMP. During the equilibration period, the simulation box expanded substantially in  $x$  and  $y$  directions and contracted in  $z$  direction to  $l_z = 3.3$  nm. Figure 8 shows the "density profiles" in the  $z$  direction. The "polymer layer" (in the center) and the "solvent layer" are clearly visible. The profiles of sulfur atoms and counterion distributions show that the  $SO_3^-$  groups are concentrated at the DMMP-polymer interface, as they are in hydrated Nafion. Unlike water, DMMP is unable to donate a hydrogen bond. It is a poor solvent for the cations, causing  $-SO_3^- K^+$  groups to associate as described in section V.3. It is also clear that DMMP is partly dissolved in the perfluoroether phase. In this simulation, we were unable to estimate the solubility, as the polymer film was too thin. However, it is reasonable to assume that in Nafion membranes DMMP would dissolve in the perfluoroether and also form small aggregates (or clusters) of solvent molecules interacting with  $-SO_3^- K^+$  via electrostatic forces.

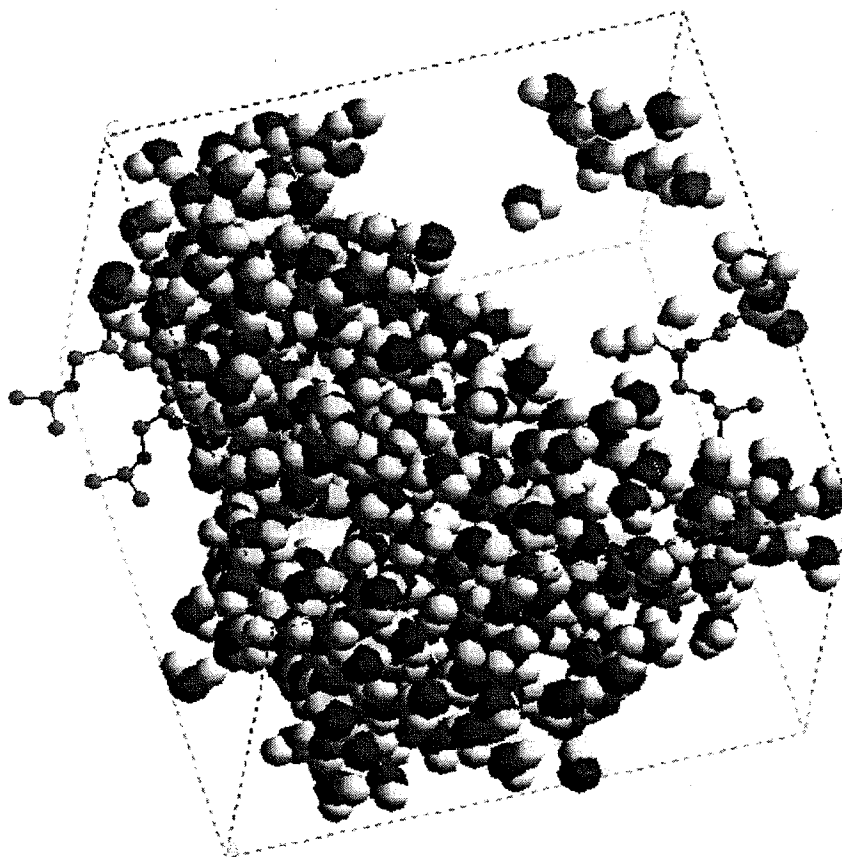
For comparison, we performed a similar simulation with the solvent bath composed of 1000 water molecules. In this case, the film-like morphology of the system was unchanged. We

found no water inside the polymer film, but we observed the formation of a water channel with several  $-SO_3^-$  groups and counterions located inside the channel. The  $SO_3^- K^+$  groups were mostly dissociated, as they were in the simulations of individual side chains with water (Figure 6).

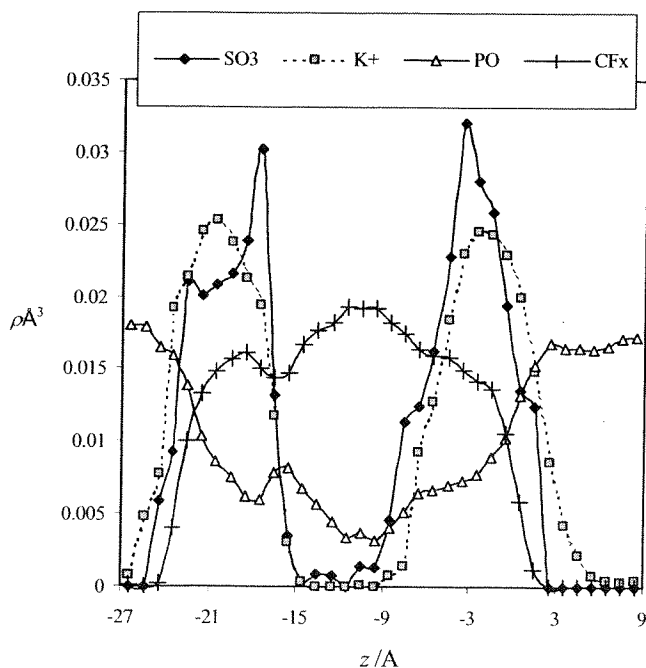
**V.5. Interaction of a Thin Nafion Film with DMMP-Water Mixture.** In practical situations, the protective membrane is nearly saturated with water, whereas the concentration of organophosphorus compounds is rather low. For this reason, we explored a Nafion film in contact with the solvent bath of 664 water molecules and 42 molecules of DMMP (total volume fraction of DMMP in solvent of 33%). The simulations were similar to those with pure components.

Figure 9 shows the snapshot of the mixture in contact with the polymer film. Surprisingly, we did not find any substantial dissolution of DMMP in the polymer phase. Rather, DMMP molecules were located at the interface between the hydrophilic and hydrophobic subphases. Certainly, in this case, it is difficult to characterize the interface and the location of DMMP molecules, since the shape of the interface is relatively rough and its location is often unclear. To analyze the morphology of the subphases, each point of the simulation cell at a particular time should be assigned to either the aqueous or the organic subphase. The connectivity of the hydrophilic subphase was checked similarly to ref 19: Any two water molecules, counterions, or  $-SO_3^-$  group separated by a distance smaller than  $l_{\text{bond}} = 3.5$  Å were assigned to the same hydrophilic aggregate. It is clear that the hydrophilic subphase was continuous over the whole course of averaging.

The radial distribution functions between the sulfur atoms of Nafion side chains and the components of the solute show that  $-SO_3^-$  groups are surrounded with water and are not obstructed by DMMP (Figure 10). A comparison of S- $O_w$  and S-P RDFs for the Nafion film-binary solution system confirms this conclusion also. However, the relative location of DMMP needs to be characterized by three-body correlations among DMMP, water, and fluorocarbon backbone, rather than by RDFs alone. For this purpose, we calculated a number of simultaneous contacts of DMMP molecules with water molecules and the backbone. A DMMP molecule was considered to belong to the hydrophilic subphase if it formed at least one hydrogen bond to a water molecule or a counterion, and to the hydrophobic subphase if any of its methyl groups had a fluorocarbon group in its close vicinity, that is 4.4 Å. Two oxygen atoms were considered to be connected by a hydrogen bond via a hydrogen atom if the distance between them did not exceed 3.4 Å and the OHO angle exceeded 90°. It was found that only about 1% (average) of DMMP molecules belonged exclusively to the hydrophobic subphase. For example, the final configuration did not contain a single DMMP molecule that was submerged into the hydrophobic subphase. About 4% of DMMP molecules belonged neither to the hydrophilic nor to the hydrophobic subphase. That is, they were surrounded by other DMMP molecules or located in the centers of DMMP mini-clusters that were observed in that system. Finally, 72% of the DMMP molecules belonged to both hydrophilic and hydrophobic subphases, and 23% were "dissolved" in water, i.e., had a hydrogen bond to a water molecule, but no neighbors among fluorocarbon groups of the backbone. The results described above suggest that DMMP tended to be located at the interface between water and Nafion. Since the radial distribution functions between the sulfur atoms of Nafion side chains and the components of the solute show that S- $O_w$  RDFs for Nafion film-water, Nafion side chains-binary solution, and Nafion



**Figure 7.** Separation of water-DMMP solution (33% vol DMMP) in the presence of model Nafion side chains. DMMP is not shown. Hydrogen in white, water oxygen in dark gray, sulfur in light gray balls. The "tails" of the model side chains are shown in sticks. It is seen that the tails are submerged in the DMMP subphase, whereas the "head" ( $-\text{SO}_3^-\text{K}^+$ ) groups are submerged in water.



**Figure 8.** Concentration profiles of different "species" in the direction of  $z$  axis (normal to the film) in the Nafion-DMMP system. The concentration of P atoms of DMMP is scaled by a factor of 3 and the concentration of ions is scaled by factor 20 in order to keep a convenient scale.

film-binary solution systems are nearly identical, it is reasonable to assume that  $-\text{SO}_3^-$  groups either occupy different places at the surface than DMMP, or they are located farther from the

surface, i.e., submerged in water. These tendencies are demonstrated qualitatively by the snapshots in Figure 9.

The results of molecular simulations show at least two important differences in segregation in membranes solvated in pure DMMP and DMMP-water mixture. First, the ionic groups that are associated in pure DMMP tend to dissociate as water is added. On the other hand, in excess water, DMMP tends to form a distinct surface layer between the subphases, around the side chains of Nafion that are terminated by  $-\text{SO}_3^-$  groups located in water. Obviously, DMMP is able to diffuse in this binary layer, whereas in the dry membrane, it may have to find its way around the hydrophobic backbone.

## VI. Conclusions

Nafion exhibits high water vapor permeability and substantial permselectivity for water and DMMP in independent measurements with the two liquids, but when measurements are conducted with mixed vapor challenge, there are interaction effects that cannot be predicted from results with the individual vapors. Most unexpected is the large reduction in water flux over the full range of water activities in the presence of DMMP vapor, even at low DMMP activity. The reduction in water permeation occurs even though DMMP causes an increase in water sorption. Similar effects of propanol on water flux occur in propanol water mixtures. Water increases the flux of DMMP only in co-current flow at moderate activities but increases the flux of propanol in both co-current and countercurrent flows. Striking improvements in DMMP barrier performance are obtained by  $\text{Ca}^{2+}$  or  $\text{Fe}^{3+}$  ion substitution of Nafion with a modest reduction in water flux, in measurements conducted with individual solvents. However, in mixed vapor measurements

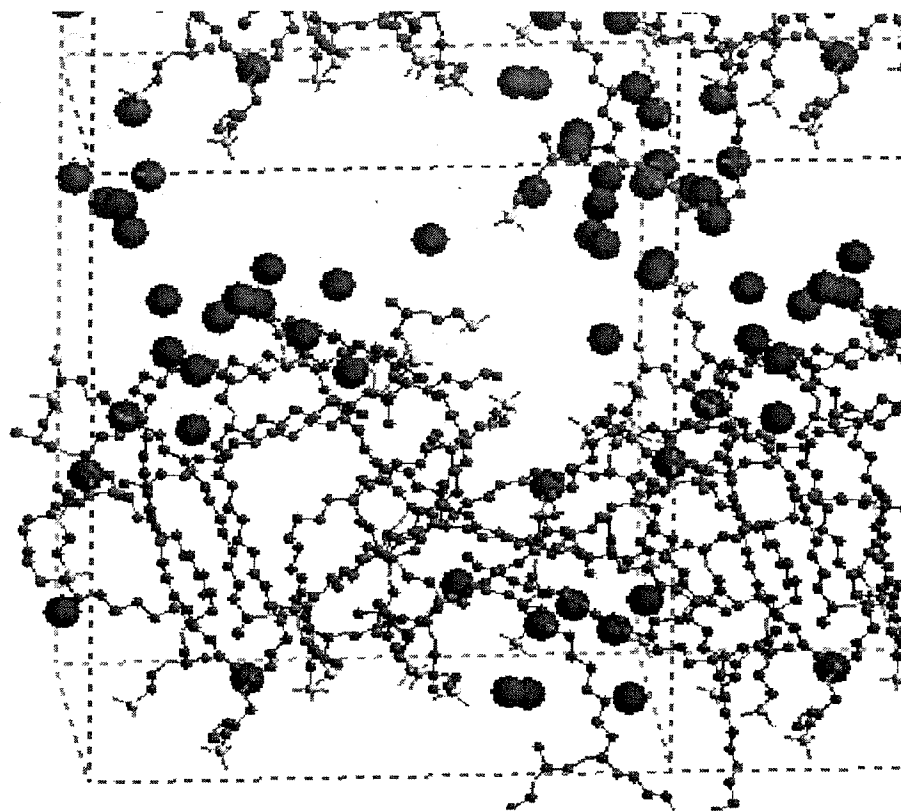


**Figure 9.** Nafion film in contact with water-DMMP mixture. Water is omitted for clarity. Gray balls denote water phosphorus atoms of DMMP, the polymer is shown in stick-ball style. DMMP prefers to locate at the interface between water and polymer.

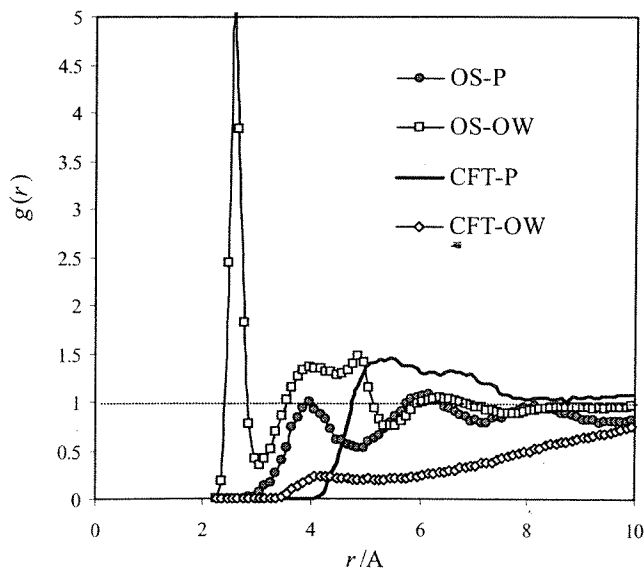


**Figure 10.** Radial distribution functions showing the separation of DMMP-water solution in the presence of model Nafion side chains. CFT is the “very tail” carbon atom of the side chain (extreme left of eq 2);  $O_S$  is the oxygen of the  $-\text{SO}_3^- \text{K}^+$  group,  $O_w$  is water oxygen, and P is the phosphorus atom of DMMP.

with these Nafion salts, DMMP causes an additional reduction in water flux at high activities, whereas, water increases transport of DMMP.

Molecular dynamics simulation of water/DMMP interactions with Nafion provides an insight into how competitive solvents effect solubility and transport behavior in the phase segregated ionomer. Simulations were conducted for a thin film model formed from six oligomers consisting of four repeat units of

the potassium sulfonate terminated fluoroether side chain with associated fluorocarbon backbone. In the absence of water, DMMP dissolves almost completely in the fluoroether phase. DMMP does not solvate the free cation but causes association of  $-\text{SO}_3^- \text{K}^+$  end groups. Water is concentrated exclusively in the ionic regions and does not mix with the fluoroether phase. Water causes ionization of the potassium sulfonate salt and forms ionic channels at the interface with the fluoroether side chains. In the mixed solvent system, containing excess water, redistribution of DMMP occurs. At the low DMMP concentration treated in the molecular modeling, over 70% of DMMP is located at the interface of the side chain phase in contact with water and more than 20% is dissolved in water, with less than 4% dissolved in the interior of the fluoroether phase.

The molecular modeling provides a basis for understanding the effect of DMMP water interactions on the permeation behavior. In the absence of water, DMMP transport occurs exclusively within dispersed fluoroether regions governed by side chain mobility, with long range transport determined primarily by tortuosity.<sup>23</sup> In the mixed solvent, DMMP redistribution to the hydrophilic interface and solution in the aqueous phase causes enhanced DMMP transport in co-current flow via water solvated ionic pathways and solution in the more mobile aqueous environment. In counter current flow, the benefits associated with the water are offset by the opposing concentration gradients, water concentration is smallest where DMMP concentration is highest, and the opposing direction of the flows. Water transport occurs solely in an aqueous phase surrounding hydrated sulfonate end groups. The reduction of water flux by DMMP can be attributed to the association of water with DMMP at the fluoroether interface and a decrease in the fraction of free water in the aqueous solution. It is likely that the polar

water containing channels are narrowed by intrusion of DMMP at the interface and by extensive swelling of the fluoroether phase at high concentrations of DMMP.

Although the present modeling is developed under conditions of dilute DMMP and high water concentrations, some of the conclusions of the single solvent and mixed solvent systems can be extended to higher DMMP concentrations. Experimental water DMMP mole ratios in the mixed liquid or mixed vapor are characteristically much higher than the ratio in the sorbed composition (Table 1), suggesting the tendency for DMMP and water to solvate separate Nafion regions with relatively little intermixing. This conclusion is supported by DMMP uptake from the mixed vapor, which is equal to the values calculated from the isotherm, whereas water concentrations are higher than isotherm predictions. Accordingly, at higher DMMP concentrations, the solution of DMMP in the fluoroether phase should predominate over preferential concentration at the hydrophilic interface. Nonetheless, the availability of facile transport at the interface and within aqueous ionic regions should continue as a significant pathway for diffusion. There are additional structural transitions in highly swollen Nafion at DMMP concentrations above 30 wt % in the absence of water, significantly above that in the film simulation model, that lead to an increase in diffusion coefficient.<sup>23</sup>

Although the modeling was concerned only with the K<sup>+</sup> form of Nafion, it is possible to apply some of the conclusions to multivalent cation modified Nafions. Since phase segregation in Nafion is driven by immiscibility of ionic and fluorocarbon regions of the polymer chain, note that the sulfonyl fluoride precursor is not phase segregated, the decreased DMMP transport observed for the Ca<sup>2+</sup> and Fe<sup>3+</sup> salts of Nafion could arise from the effect of charge shielding on phase segregation. Also, multivalent cations acting as ionic cross links are expected to force closer proximity of sulfonate groups limiting fluoroether side chain mobility. In the absence of water, DMMP solvates -SO<sub>3</sub><sup>-</sup> K<sup>+</sup> but does not produce ionization of the salt and should interact similarly with Ca<sup>2+</sup> and Fe<sup>3+</sup> salts. The loss of DMMP resistance at high water concentrations can be attributed to a combination of factors. Water promotes hydrolysis of the multivalent cation salts, reducing constraints on side chain mobility, and DMMP redistributes to pathways of enhanced mobility and extended continuity at the aqueous interface. However, DMMP permeation is low in the Nafion salts at water activity <0.9, and it is the marked reduction in water flux associated with cation modification and DMMP exposure which limits permselective barrier performance.

There are qualitative similarities but equally significant differences in the effect of propanol-water mixtures on the respective fluxes. In the absence of water, propanol solvates the sulfonate group as shown by a decrease in solubility in going from acid to salt forms and also dissolves in the fluoroether phase with an increase in segmental motion by analogy to results of NMR line narrowing measurements in Nafion swollen with ethanol.<sup>10</sup> There is also the possibility of propanol dissolving to a small extent in the fluorocarbon phase, based on molecular dynamics simulation predictions of methanol interaction with the fluorocarbon backbone<sup>9</sup> and NMR observations of a small increase in mobility of fluorocarbon regions with ethanol.<sup>10</sup> Thus, the diffusion of propanol, even in the absence of water, should be less restricted by fluorocarbon structure than in the case of DMMP. In sorption from the mixed vapor, propanol concentrations are decreased below those predicted by the pure vapor isotherm while sorbed water is increased. Accordingly, the pronounced increase in propanol flux and reduction in water

flux with mixed vapor cannot be explained as due simply to solubility changes for either component. Significant interactions between water and propanol must occur to enhance the flux of propanol and retard the flux of water. Propanol would be expected to primarily solvate the fluoroether phase even in sorption from mixed solvent. However, since propanol, unlike DMMP, is a protic solvent, water should also dissolve in the propanol-swollen fluoroether phase. This suggestion is supported by mole ratio values for water-propanol. In contrast to water-DMMP values, mole ratios for water-propanol in the mixed liquid or mixed vapor and in the sorbed composition are essentially equal, indicating mutual solvation resulting in less distinct compositional differences in the aqueous and fluoroether phases. Propanol transport would occur across the extended solvated region, whereas water transport would be diminished by mixing with propanol in the fluoroether phase and by interactions in the aqueous ionic regions. Redistribution of propanol to the fluoroether aqueous interface and solution in the aqueous ionic regions can occur, as proposed for DMMP water mixtures, but would play a much smaller role in the transport behavior.

The results of this study show that solubility and transport in mixed solvent systems in the phase segregated fluoroionomer, Nafion, cannot be predicted from measurements conducted with the individual solvents but must take into account complex interactions which can affect the distribution between the aqueous and fluoroether phases. For example, absorption of pure solvents by Nafion gives two distinct swelling envelopes with maxima near 10 and 17 Hb when plotted against solubility parameter, but aqueous solutions give a single broad maximum shifted toward 17 Hb.<sup>24,25</sup> The present study shows that the solubility from aqueous mixtures is not determined solely by solvent compatibility but results from competitive interactions between solvent molecules and the segregated phases of the polymer as demonstrated by comparison of sorbed concentrations from mixed aqueous solvent vapors. This is amplified in the key finding of the simulation modeling which, for the individual solvents shows that DMMP and water solvate separate regions of Nafion. In the mixed solvent system, modeling reveals a redistribution of DMMP to the aqueous interfacial region and associated ionic channels. This demonstrates the unique and necessary contribution that molecular modeling can make to an understanding of transport behavior with mixed solvents in phase segregated polymers.

**Acknowledgment.** The work is supported by USARO, grant DAAD 190110545.

## References and Notes

- (1) Porat, Z.; Fryer, J. R.; Huxham, M.; Rubinstein, I. *J. Phys. Chem.* **1995**, *99*, 4667.
- (2) Ludvigsson, M.; Lindgren, J.; Tegenfeldt, J. *Electrochim. Acta* **2000**, *45*, 2267.
- (3) Rollet, A. L.; Diat, O.; Gebel, G. *J. Phys. Chem. B* **2002**, *106*, 3033.
- (4) Paddison, S. J. *Annu. Rev. Mater. Res.* **2003**, *33*, 289.
- (5) Kato, S.; Nagahama, K.; Noritomi, H.; Asai, H. *J. Membr. Sci.* **1992**, *72*, 31.
- (6) Xie, G.; Okada, T. *J. Electrochem. Soc.* **1995**, *142*, 3057.
- (7) Ye, X.; LeVan, D. *J. Membr. Sci.* **2003**, *221*, 147.
- (8) Paul, R. L.; Lindstrom, R. M. *J. Radioanal. Nuclear Chem.* **2000**, *243*, 181.
- (9) Vishnyakov, A.; Neimark, A. V. *J. Phys. Chem. B* **2000**, *104*, 4471.
- (10) Meresi, G.; Wang, Y.; Bandis, A.; Inglefield, P. T.; Jones, A. A.; Wen, W. Y. *Polymer* **2001**, *42*, 6153.
- (11) Giotto, M. V.; Zhang, J. H.; Inglefield, P. T.; Wen, W. Y.; Jones, A. A. *Macromolecules* **2003**, *36*, 4397.
- (12) Rivin, D.; Kendrick, C. E.; Gibson, P. W.; Schneider, N. S. *Polymer* **2001**, *42*, 623.

- (13) Rivin, D.; Schneider, N. S.; Gibson, P. W.; Kendrick, C. E. 7th International symposium on Protection, 2001, Stockholm.
- (14) Vishnyakov, A.; Neimark, A. V. *J. Phys. Chem. B* **2001**, *105*, 7830.
- (15) Nandan, D.; Mohan, H.; Iyer, R. M. *J. Membr. Sci.* **1992**, *71*, 69.
- (16) Accelrys, I. Cerius2; 4.2 ed.; Accelrys Inc: San Diego, CA, 2000.
- (17) Berendsen, H. J. C.; Grigera, J. R.; Straatsma, T. P. *J. Phys. Chem.* **1987**, *91*, 6269.
- (18) Vishnyakov, A.; Neimark, A. V. *J. Phys. Chem. A* **2003**, in press.
- (19) Vishnyakov, A.; Neimark, A. V. *J. Phys. Chem. B* **2001**, *105*, 9586.
- (20) Watkins, E. K.; Jorgensen, W. L. *J. Phys. Chem. A* **2001**, *105*, 4118.
- (21) Elliott, J. A.; Hanna, S.; Elliott, A. M. S.; Cooley, G. E. *Phys. Chem. Chem. Phys.* **1999**, *1*, 4855.
- (22) Heinzinger, K. *Physica B C* **1985**, *131*, 196.
- (23) Yeo, R. S.; Cheng, C. H. *J. Appl. Polym. Sci.* **1986**, *32*, 5733.
- (24) Schneider, N. S.; Rivin, D. *Polymer* **2003**, submitted.
- (25) Yeo, R. S. *Polymer* **1980**, *21*, 432-435.